

# Vortical effects in chiral band structures

Swadeepan Nanda<sup>1</sup> and Pavan Hosur<sup>1</sup>

<sup>1</sup>University of Houston, Houston, TX

(Dated: June 29, 2022)

The chiral vortical effect is a chiral anomaly induced transport phenomenon characterized by an axial current in a uniformly rotating chiral fluid. It is well-understood for Weyl fermions in high energy physics, but its realization in condensed matter band structures, including those of Weyl semimetals, has been controversial. In this work, we develop the Kubo response theory for electrons in a general band structure subject to space- and time-dependent rotation or vorticity relative to the background lattice. We recover the chiral vortical effect in the static limit; in the transport or uniform limit, we discover a new effect that we dub the gyrotropic vortical effect. The latter is governed by Berry curvature of the occupied bands while the former contains an additional contribution from the magnetic moment of electrons on the Fermi surface. The two vortical effects can be understood as analogs of the well-known chiral and gyrotropic magnetic effects in chiral band structures. We address recent controversies in the field and conclude by describing device geometries that exploit Ohmic or Seebeck transport to drive the vortical effects.

*Introduction.*— Chiral transport phenomena in three dimensions have garnered tremendous interest in condensed matter physics since the discovery of Weyl semimetals (WSMs) – three dimensional topological materials defined by the presence of accidental intersections between non-degenerate bands [1–19]. Near these intersections or Weyl nodes, the Hamiltonian resembles that of massless, relativistic Weyl fermions. Weyl nodes have a well-defined handedness or chirality and behave like unit magnetic monopoles for Berry flux in momentum space. Chiral transport phenomena in WSMs are characterized by distinct responses of right- and left-handed Weyl fermions to external perturbations such as electromagnetic fields and can invariably be traced to the chiral anomaly, defined as the violation of the classical  $U(1)$  chiral gauge symmetry by the quantum path integral [20]. Although the anomaly, first discovered in high-energy physics, is strictly absent in WSMs as they necessarily contain equal numbers of right- and left-handed Weyl nodes [21, 22], clever ways of resolving the nodes have led to a myriad of anomalous behaviors of WSMs subject to electromagnetic fields [23–40].

Fundamentally, the anomaly manifests as a non-conservation of chiral charge in the presence of parallel electric and magnetic fields even though the low energy Weyl Hamiltonian naïvely predicts chiral charge conservation. Alternately, it generates the chiral magnetic effect (CME), defined as an equilibrium, dissipationless current along a constant magnetic field:  $\mathbf{j} \propto \mathbf{B}$  [41, 42]. Such a current is allowed in the continuum, where purely left-handed (or purely right-handed) Weyl fermions can exist. However, similarly to the anomaly, the CME too is forced to vanish in WSMs due to lattice regularization. The core difference between the continuum and the lattice versions of the CME generated great debate during its adaptation from high-energy to condensed matter physics [27, 28, 43–47]. The controversies were eventually resolved by extending the response to non-zero frequency

( $\omega$ ) and momentum ( $\mathbf{q}$ ) and distilling subtleties of the dc limit. The *static* limit ( $\omega \rightarrow 0$  before  $q \rightarrow 0$ ) leads to a non-zero CME only if the system is held in a non-equilibrium steady state and directly measures the Berry monopole charge enclosed by the occupied states [48, 49]. In contrast, the *uniform* limit ( $q \rightarrow 0$  before  $\omega \rightarrow 0$ ) was termed the gyrotropic magnetic effect (GME) [48] and was shown to describe the equilibrium response to a time-dependent magnetic field, or equivalently, a circulating electric field:  $\mathbf{j} \propto \nabla \times \mathbf{E}$ . Interestingly, it can exist even in band structures that lack Weyl nodes but break time-reversal ( $\mathcal{T}$ ) and inversion ( $\mathcal{I}$ ) symmetries.

The chirality, however, is an intrinsic property of the Weyl Hamiltonian that does not rely on coupling to electromagnetic fields. A natural question is, “what chiral transport phenomena do neutral Weyl fermions exhibit?” A striking such response is the chiral vortical effect (CVE), defined as the appearance of a dissipationless axial current in a rotating Weyl fluid. It was initially predicted for neutrino fluxes from rotating black holes and other chiral relativistic field theories [40, 41, 50–61] and has been observed in heavy-ion collisions [62]. It is usually described as a CME where the Coriolis force in a rotating frame simulates  $\mathbf{B}$ . However, it differs from the CME in key ways. Firstly, it is more fundamental as it is a strictly kinematic effect that does not rely on gauge fields. Secondly, it is much less understood in condensed matter; its historical derivations using Boltzmann and hydrodynamic equations have yielded elegant solutions in the static limit, especially for Lorentz invariant Weyl fermions [40, 54–61, 63–66], but its generalization to arbitrary band structures at finite  $\mathbf{q}$  and  $\omega$  remains an open problem. Thirdly, electrons under a static  $\mathbf{B}$  are within the purview of Bloch’s theorem that forbids an equilibrium current in an infinite system [67–69], but the theorem is inapplicable for a fluid rotating at constant angular velocity. We will return to this point later. Finally, both lattice and continuum realizations of the CME

can be triggered in practice by merely applying a suitable  $\mathbf{B}$ . In contrast, a continuous fluid can be physically rotated to trigger the CVE, but crystalline solids do not provide a mechanical handle for rotating the electrons in their bands. A practical route to rotate the electrons in a solid is essential for harnessing the phenomenon for device applications.

In this work, we develop the theoretical framework for describing the current response of electrons in a general band structure rotated relative to a stationary lattice at a space- and time-dependent angular velocity  $\boldsymbol{\Omega}(\mathbf{r}, t)$ . Alternately, the current can be interpreted as a response to space and time-dependent vorticity  $\boldsymbol{\mathcal{V}}(\mathbf{r}, t) = \nabla \times \mathbf{u}(\mathbf{r}, t)/2$ , where  $\mathbf{u}(\mathbf{r}, t)$  is the velocity field of the electron fluid. This is because, for smooth and slow dependence on  $\mathbf{r}$  and  $t$ ,  $\mathbf{u}(\mathbf{r}, t) = \boldsymbol{\Omega}(\mathbf{r}, t) \times \mathbf{r}$  immediately yields  $\boldsymbol{\mathcal{V}}(\mathbf{r}, t) = \boldsymbol{\Omega}(\mathbf{r}, t)$ . In other words, the vorticity locally mimics angular velocity about the vortex axis.

We will focus on the static and uniform limits, which respectively describe the response to time-independent and time-dependent spatially uniform vorticity or angular velocity. The static limit corresponds to the CVE while the uniform limit gives a new response that we term the gyrotropic vortical effect (GVE). The GVE can be viewed as a response to angular acceleration,  $\boldsymbol{\alpha}(\mathbf{r}, t) = \partial_t \boldsymbol{\Omega}(\mathbf{r}, t)$ , but its gyrotropic nature becomes transparent when viewed as the response to circulating acceleration  $\nabla \times \mathbf{a}(\mathbf{r}, t) \equiv \nabla \times \partial_t \mathbf{u}(\mathbf{r}, t)$ . Thus, just as the CVE is usually interpreted as the rotational analog of the CME, the GVE proposed here can be understood as the rotational or vortical counterpart of the GME.

Microscopically, we show that the GVE stems from purely interband virtual processes whereas the CVE relies on both interband and intraband processes. In other words, we show that the relevant linear response functions are given by

$$\chi^{\text{CVE}} = \chi^{\text{stat}} = \chi^{\text{intra}} + \chi^{\text{inter}} \quad (1a)$$

$$\chi^{\text{GVE}} = \chi^{\text{uni}} = \chi^{\text{inter}} \quad (1b)$$

Eqs. (1) summarize our main results. Explicit expressions for  $\chi^{\text{inter}}$  and  $\chi^{\text{intra}}$  that are valid for general band structures are given later in Eqs. (9) and (11), while Fig. (1) illustrates the corresponding microscopic processes for a WSM with Weyl nodes at different energies.

*Vortical response theory:-* We now develop the vortical response theory and derive expressions for  $\chi^{\text{intra}}$  and  $\chi^{\text{inter}}$ . We begin by imagining electrons governed by a Bloch Hamiltonian  $H_0(\mathbf{k})$  driven in such a way that they rotate by a space- and time-dependent angular velocity  $\boldsymbol{\Omega}(\mathbf{r}, t)$ . For  $\boldsymbol{\Omega}(\mathbf{r}, t)$  varying slowly in space and time and ignoring rotation of the wavefunction within a unit cell, the local dynamics are governed by the time-dependent Schrodinger equation for the Hamiltonian  $H'(\mathbf{k}, \mathbf{r}, t) = U(\mathbf{r}, t)H_0(\mathbf{k})U^\dagger(\mathbf{r}, t)$  where  $U(\mathbf{r}, t) = \exp\left[-i \int_0^t \mathbf{L} \cdot \boldsymbol{\Omega}(\mathbf{r}, t') dt'\right]$  and  $\mathbf{L} = \mathbf{r} \times \mathbf{k}$  is the spatial

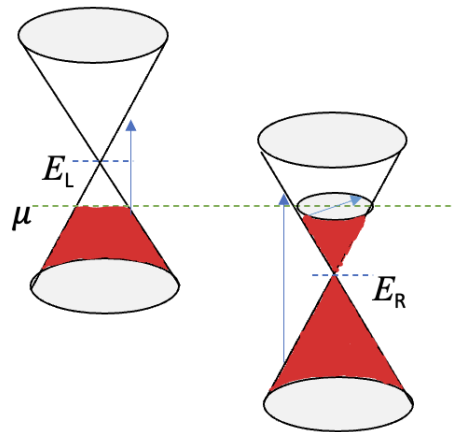


FIG. 1. Schematic of microscopic processes causing the vortical effects in a WSM with left- and right-handed Weyl nodes at different energies. The GVE arises from non-resonant ( $E_{\mathbf{k}}^m - E_{\mathbf{k}}^n \neq \omega$ ) interband ( $m \neq n$ ) virtual processes at  $q = 0$  (vertical arrows) and survives as  $\omega \rightarrow 0$  provided  $E_L \neq E_R$ . The CVE appears in the static limit  $\omega = 0$ ,  $q \rightarrow 0$ , and contains an additional contribution from intraband ( $m = n$ ) resonant ( $E_{\mathbf{k}}^n = E_{\mathbf{k}+\mathbf{q}}^n$ ) processes (horizontal arrow).

angular momentum (in units  $\hbar = 1$ ) that generates rotations on long length scales compared to the lattice constant. Equivalently, the wavefunction in a frame rotating at  $\boldsymbol{\Omega}(\mathbf{r}, t)$ ,  $\psi_{\text{rot}} = U^\dagger(\mathbf{r}, t)\psi_{\text{lab}}$ , is governed by the Hamiltonian

$$H(\mathbf{k}, \mathbf{r}, t) = H_0(\mathbf{k}) - \mathbf{L} \cdot \boldsymbol{\Omega}(\mathbf{r}, t) \quad (2)$$

This yields the kinematic or paramagnetic current operator in the lab frame,  $\mathbf{j}(\mathbf{k}, \mathbf{r}, t)$ :

$$\mathbf{j}(\mathbf{k}, \mathbf{r}, t) = e[\nabla_{\mathbf{k}} H(\mathbf{k}, \mathbf{r}, t) + \mathbf{u}(\mathbf{r}, t)] = e\mathbf{v}_{\mathbf{k}} \equiv \mathbf{j}(\mathbf{k}) \quad (3)$$

where  $\mathbf{v}_{\mathbf{k}} = \nabla_{\mathbf{k}} H_0(\mathbf{k})$ ,  $e < 0$  is the charge of an electron. The vortical effects are given by the linear current response to the perturbation  $-\mathbf{L} \cdot \boldsymbol{\Omega}(\mathbf{r}, t)$ , which can be computed using the Kubo formula.

A subtlety arises, however, since  $\mathbf{L}$  is not translationally invariant yet the corresponding vertex conserves momentum because  $\mathbf{r} \equiv i\nabla_{\mathbf{q}}\delta(\mathbf{q} - \mathbf{q}')$ . To incorporate the derivative of the Dirac delta function properly, we must consider the Fourier momenta of  $\boldsymbol{\Omega}(\mathbf{r}, t)$  to be smoothly distributed over a small range, e.g.,  $\boldsymbol{\Omega}(\mathbf{q}', \omega) = \text{const}$  for  $|\mathbf{q} - \mathbf{q}'| < \epsilon$  and zero for  $|\mathbf{q} - \mathbf{q}'| > \epsilon$ , where  $\epsilon$  is a small positive number. The Kubo formula then gives

$$\langle j_\alpha(\mathbf{q}, i\omega_n) \rangle = \int_{\mathbf{q}'} \tilde{\chi}_{\alpha\beta}(\mathbf{q}, \mathbf{q}', i\omega_n) \Omega_\beta(\mathbf{q}', i\omega_n) \quad (4)$$

as a function of Matsubara frequencies, where

$$\tilde{\chi}_{\alpha\beta}(\mathbf{q}, \mathbf{q}', i\omega_n) = -T \sum_{\mathbf{k}, i\nu_n} \text{tr} [j_\alpha(\mathbf{k}, \mathbf{q}') G(\mathbf{k}, i\nu_n) \times L_\beta(\mathbf{k}, \mathbf{q}', \mathbf{q}) G(\mathbf{k} + \mathbf{q}', i\nu_n + i\omega_n)] \quad (5)$$

where  $G(\mathbf{k}, i\nu_n) = [i\nu_n - H_0(\mathbf{k})]^{-1}$  as usual and

$$\mathbf{L}(\mathbf{k}, \mathbf{q}', \mathbf{q}) = (2\pi)^3 i \nabla_{\mathbf{q}'} \delta(\mathbf{q} - \mathbf{q}') \times \mathbf{k} \quad (6)$$

The form of  $\mathbf{L}$  in momentum space ensures only  $\mathbf{q}' = \mathbf{q}$  contributes to  $\langle j_\alpha(\mathbf{q}, i\omega_n) \rangle$ . Integrating over  $\mathbf{q}'$ , summing over Matsubara frequencies and analytically continuing the driving frequency give the retarded response function  $\chi_{\alpha\beta}(\mathbf{q}, \omega) = \int_{\mathbf{q}'} \tilde{\chi}_{\alpha\beta}(\mathbf{q}, \mathbf{q}', i\omega_n \rightarrow \omega + i0^+)$ :

$$\chi_{\alpha\beta}(\mathbf{q}, \omega) = - \int_{\mathbf{k}} (\mathbf{k} \times i \nabla_{\mathbf{q}})_\beta \sum_{m,n} \frac{f(E_{\mathbf{k}}^m) - f(E_{\mathbf{k}+\mathbf{q}}^n)}{E_{\mathbf{k}}^m - E_{\mathbf{k}+\mathbf{q}}^n + \omega} \mathcal{J}_{\alpha\mathbf{k}}^{nm} \mathcal{U}_{\mathbf{k}}^{mn}(\mathbf{q}) \quad (7)$$

where  $\mathcal{J}_{\alpha\mathbf{k}}^{nm} = \langle u_{\mathbf{k}+\mathbf{q}}^n | j_\alpha(\mathbf{k}) | u_{\mathbf{k}}^m \rangle$ ,  $\mathcal{U}_{\mathbf{k}}^{mn}(\mathbf{q}) = \langle u_{\mathbf{k}}^m | u_{\mathbf{k}+\mathbf{q}}^n \rangle$ ,  $H_0(\mathbf{k}) | u_{\mathbf{k}}^n \rangle = E_{\mathbf{k}}^n | u_{\mathbf{k}}^n \rangle$  and  $f(E) = 1/[\exp(E/k_B T) + 1]$ . Eq. (7) is the general vortical response function that describes the current driven by spacetime-dependent rotation or vorticity. Henceforth, we focus on the isotropic part,  $\chi_{\text{iso}}(\mathbf{q}, \omega) = \frac{1}{3} \chi_{\alpha\alpha}(\mathbf{q}, \omega)$ , for simplicity and evaluate it in the uniform and static limits to obtain the GVE and the CVE.

*GVE in the uniform limit:-* This limit is defined by  $q \rightarrow 0$  followed by  $\omega \rightarrow 0$ . Thus, setting  $q = 0$  in Eq. (7) and extracting the isotropic part, we obtain

$$\chi_{\text{iso}}(0, \omega) = -\frac{e}{3} \sum_{m,n} \int_{\mathbf{k}} \frac{f(E_{\mathbf{k}}^m) - f(E_{\mathbf{k}}^n)}{E_{\mathbf{k}}^m - E_{\mathbf{k}}^n + \omega} \mathbf{v}_{\mathbf{k}}^{nm} \cdot (\mathbf{k} \times \mathbf{A}_{\mathbf{k}}^{mn}) \quad (8)$$

where  $\mathbf{A}_{\mathbf{k}}^{mn} = i \langle u_{\mathbf{k}}^m | \nabla_{\mathbf{k}} u_{\mathbf{k}}^n \rangle$  and  $\mathbf{v}_{\mathbf{k}}^{nm} = \langle u_{\mathbf{k}}^n | \mathbf{v}_{\mathbf{k}} | u_{\mathbf{k}}^m \rangle$ . The intraband ( $m = n$ ) contributions vanish since  $\omega \neq 0$ , so the effect in this regime is purely due to interband processes. Using  $\mathbf{v}_{\mathbf{k}}^{nm} = i \mathbf{A}_{\mathbf{k}}^{nm} (E_{\mathbf{k}}^n - E_{\mathbf{k}}^m)$  for  $m \neq n$ , the  $\omega \rightarrow 0$  limit simplifies to

$$\chi^{\text{uni}} = \chi^{\text{inter}} = \frac{2e}{3} \sum_n \int_{\mathbf{k}} f(E_{\mathbf{k}}^n) \mathbf{F}_{\mathbf{k}}^n \cdot \mathbf{k} \quad (9)$$

where  $\mathbf{F}_{\mathbf{k}}^n = i \langle \nabla_{\mathbf{k}} u_{\mathbf{k}}^n | \times | \nabla_{\mathbf{k}} u_{\mathbf{k}}^n \rangle$  is the Berry curvature of the  $n^{\text{th}}$  band. In analogy with the GME, we term this effect the GVE. It vanishes in systems with  $\mathcal{I}$  symmetry which forces  $\mathbf{F}_{\mathbf{k}}^n = \mathbf{F}_{-\mathbf{k}}^n$ , but is generically non-zero in  $\mathcal{I}$ -breaking,  $\mathcal{T}$ -symmetric systems, which obey  $\mathbf{F}_{\mathbf{k}}^n = -\mathbf{F}_{-\mathbf{k}}^n$ . Naïvely,  $\chi^{\text{uni}}$  seems poorly regularized as it receives contributions from all occupied states. However, the total contribution from a filled band vanishes at  $T = 0$  in the continuum limit, when the Brillouin zone can be

compactified to a sphere and all points at  $k \rightarrow \infty$  are identified. Specifically,  $\int_{BZ} \mathbf{F}_{\mathbf{k}}^n \cdot \mathbf{k} = \int_{\partial BZ} (\mathbf{A}_{\mathbf{k}}^n \times \mathbf{k}) \cdot d\mathbf{s}$  using Gauss's divergence theorem, but the last expression vanishes since  $|u_{\mathbf{k}}^n\rangle$  must be constant on  $\partial BZ$  due to the above boundary condition. Thus, only partially occupied bands contribute to  $\chi^{\text{uni}}$ .

For an isotropic Weyl fermion of chirality  $C = \pm 1$  described by  $H_0(\mathbf{k}) = C v \mathbf{k} \cdot \boldsymbol{\tau} - \mu$ , where  $\boldsymbol{\tau}$  are Pauli matrices, the energies and Berry curvatures for the  $n = \pm 1$  bands are  $E_{\mathbf{k}}^n = n v k - \mu$  and  $\mathbf{F}_{\mathbf{k}}^n = -C n \frac{\hat{\mathbf{k}}}{2k^2}$ . Thus, for a WSM with Weyl nodes of chirality  $C_i$  and velocity  $v_i$  at energy  $E_i$ ,  $i = 1 \dots 2N$ , and chemical potential  $\mu$ , Eq. (9) reduces at  $T = 0$  to

$$\chi_{\text{WSM}}^{\text{GVE}} = -\frac{e}{12\pi^2} \sum_{i=1}^{2N} C_i \left( \frac{\mu - E_i}{v_i} \right)^2 \quad (10)$$

In deriving the above, we have subtracted the contribution of undoped Weyl nodes since filled bands do not contribute, as argued earlier.

*CVE in the static limit:-* This limit is defined by  $\omega \rightarrow 0$  followed by  $q \rightarrow 0$ . Upon setting  $\omega = 0$  and taking  $q \rightarrow 0$  in Eq. (7), the isotropic part  $\chi_{\text{iso}}(\mathbf{q}, \omega)$  reduces to  $\chi^{\text{stat}} = \chi^{\text{intra}} + \chi^{\text{uni}}$ , as written in Eq. (1a), where

$$\chi^{\text{intra}} = \frac{2e}{3} \sum_n \int_{\mathbf{k}} f'(E_{\mathbf{k}}^n) \mathbf{k} \cdot \mathbf{m}_{\mathbf{k}}^n \quad (11)$$

Here,  $\mathbf{m}_{\mathbf{k}}^n = \frac{i\mathbf{e}}{2} \langle \nabla_{\mathbf{k}} u_{\mathbf{k}}^n | \times (H_{\mathbf{k}} - E_{\mathbf{k}}^n) | \nabla_{\mathbf{k}} u_{\mathbf{k}}^n \rangle$  denotes the orbital moment of the Bloch state  $|u_{\mathbf{k}}^n\rangle$ . Thus,  $\chi^{\text{stat}}$  contains one additional intraband contribution compared to  $\chi^{\text{uni}}$ , which stems from the limit  $\frac{f(E_{\mathbf{k}}^n) - f(E_{\mathbf{k}+\mathbf{q}}^n)}{E_{\mathbf{k}}^n - E_{\mathbf{k}+\mathbf{q}}^n} \xrightarrow{q \rightarrow 0} f'(E_{\mathbf{k}}^n)$ .

A Weyl fermion described by  $H_0(\mathbf{k}) = C v \mathbf{k} \cdot \boldsymbol{\tau} - \mu$  has  $\mathbf{m}_{\mathbf{k}}^n = C n \frac{\hat{\mathbf{k}}}{2k}$  and  $f'(E_{\mathbf{k}}^n) = -n \delta(vk - |\mu|)$ . For a WSM, this straightforwardly yields

$$\chi_{\text{WSM}}^{\text{intra}} = -\frac{1}{6\pi^2} \sum_{i=1}^{2N} \epsilon C_i \left( \frac{\mu - E_i}{v_i} \right)^2 \quad (12)$$

Including  $\chi^{\text{inter}} \equiv \chi_{\text{WSM}}^{\text{GVE}}$ , we obtain the CVE for WSMs,

$$\chi_{\text{WSM}}^{\text{CVE}} = -\frac{1}{4\pi^2} \sum_{i=1}^{2N} \epsilon C_i \left( \frac{\mu - E_i}{v_i} \right)^2 \quad (13)$$

Eq. (13) is the well-known expression for the CVE in relativistic Weyl fermions [40, 54–61].

*Comparisons:-* The past decade has seen growing interest in vortical effects in both relativistic and non-relativistic chiral fermions as well as in their magnetic counterparts. We now contrast our approach and results with the existing ones in each context.

Ref. [56] calculated the CVE in Lorentz invariant kinetic theories and showed that

$$\mathbf{j}^{\text{CVE}} = \frac{\mu^2}{4\pi^2 v^2} \boldsymbol{\Omega} \quad (14)$$

at  $T = 0$  for a single right-handed isotropic Weyl fermion, where  $v$  is the Weyl velocity and  $\mu$  is measured relative to the Weyl node energy. While this result is well-known, Ref. [56] showed that  $\mathbf{j}^{\text{CVE}}$  consists of two parts: a Liouville current  $\mathbf{j}_I^{\text{CVE}} = \frac{1}{3}\mathbf{j}^{\text{CVE}}$  from the group velocity of all occupied (unoccupied) states above (below) the Weyl node and a magnetization current  $\mathbf{j}_{II}^{\text{CVE}} = \frac{2}{3}\mathbf{j}^{\text{CVE}}$  from the magnetization of states near the Fermi surface. Moreover, the above separation of terms was shown to arise purely from Lorentz invariance. Interestingly, our results for a single right-handed Weyl fermion show precisely the same separation between interband and intraband terms. In particular, interband processes contribute to the Liouville current while intraband processes determine the magnetization current. Both terms exist in the static limit and yield the CVE. In contrast, the uniform or transport limit gives rise to the GVE and receives contributions from interband processes only, thus consisting purely of a Liouville current. Our Kubo formula approach provides microscopic insight into the CVE that complements the arguments in Ref. [56] based on Lorentz invariance.

For non-relativistic systems, recent works have triggered a debate regarding the correct description of vortical effects. Ref. [64] described hydrodynamic transport in non-centrosymmetric materials and included the effect of vorticity through a coupling  $-\mathbf{L} \cdot \mathbf{V}$  to the spatial angular momentum. In contrast, Ref. [63] also included a spin-vorticity coupling,  $-\mathbf{S} \cdot \mathbf{V}$ . In writing Eq. (2), we have effectively adopted the former approach. Physically, this choice describes a fluid rotating relative to a stationary lattice in such a way that its internal degrees of freedom such as spin and orbital do not directly couple to the external force driving the rotation. For instance, for flow driven by an electric field, spin-vorticity coupling is negligible because it is suppressed by the ratio of the fluid speed to the speed of light. On the other hand, if the crystal is mechanically rotated, the approach of Ref. [63] is appropriate as rotation of the underlying lattice couples to all degrees of freedom of the electron gas that lives in it. If spin-vorticity coupling is neglected, our results match with those of Ref. [63] provided our uniform and static limits are identified with their transport and magnetization currents, respectively, with an extra minus sign for the latter because we calculate the paramagnetic current whereas orbital magnetization current is diamagnetic.

Finally, we compare and contrast the results for the vortical effects with their magnetic counterparts. The magnetic and vortical effects all require broken  $\mathcal{I}$  as well as broken  $\mathcal{T}\mathcal{I}$  symmetries. However, the CME explicitly requires the presence of Weyl nodes while the GME as well as both the vortical effects can exist for general chiral band structures devoid of Weyl nodes. The microscopic contributions to the various effects are also different: the CME and the GME are governed by the net chirality

of the occupied bands and the Fermi surface magnetization, respectively. In contrast, the GVE depends on the Berry curvature of the occupied bands whereas the CVE contains additional contribution from the orbital magnetization of states on the Fermi surface.

*Implications for Bloch's theorem:-* Bloch's theorem states that the current density vanishes in the thermodynamic limit in an arbitrary system at equilibrium. In WSMs, it manifests as a vanishing equilibrium CME. To activate a CME, chiral charge first needs to be pumped across Weyl nodes to create a non-equilibrium steady-state. It is often stated that the CVE evades Bloch's theorem because the thermodynamic limit here violates causality. Specifically, if a fluid rotates at constant  $\Omega$ , particles far enough from the rotation axis will be forced to travel faster than light, so the system must necessarily have a finite size. However, a recent refinement of Bloch's theorem for finite systems shows that the current density is bounded only by the inverse system size in the current direction, i.e.,  $|\langle j_z \rangle| < O(1/l_z)$  [70]. Therefore, a generic equilibrium system must have vanishing  $|\langle j_z \rangle|$  as  $l_z \rightarrow \infty$  regardless of its transverse dimensions. This contradicts Eq. (13), which clearly predicts a non-zero CVE.

The resolution to the paradox can be understood in two equivalent ways. From the lab perspective, the energy of a fluid rotating at constant  $\Omega$  can always be lowered by slowing down its rotation, whereas Bloch's theorem assumes that the fluid is already in its lowest energy state. Alternately, the rotating frame Hamiltonian in Eq. (2) violates a key assumption of Bloch's theorem, namely, an energy spectrum that is bounded below, since  $\mathbf{L}$  is unbounded. Specifically, the upper bound on  $|\mathbf{L}| = |\mathbf{r} \times \mathbf{k}|$  is of order  $l_{\perp}/a_{\perp}$ , where  $a_{\perp}$  is the lattice constant in the  $i$ -direction, which diverges in both continuum ( $a_{\perp} \rightarrow 0$ ) and thermodynamic ( $l_{\perp} \rightarrow \infty$ ) limits in the transverse directions.

*Device geometries:-* We close by sketching various device geometries that rely on the vortical effects. In these devices, carriers are forced to traverse curved paths by a combination of device geometry and electromagnetic or thermal fields and hence, endowed with a non-zero  $\Omega$  relative to the background lattice. As a result, they develop a voltage perpendicular to the plane of motion. Figs. 2(a)-(c) illustrate the basic ideas for vortical effects driven by an electric field, thermal gradient and time-dependent magnetic flux, respectively. If the mobility is  $\mu_{\text{mob}}$  and the radius of the curved path is  $R$ , an electric field  $E$  induces a drift velocity  $v_d = \mu_{\text{mob}}E$  and hence,  $\Omega = \mu_{\text{mob}}E/R$ . Assuming typical values for a WSM,  $E = 0.1V/m$ ,  $R = 1\mu m$ ,  $\mu_{\text{mob}} = 10^5 cm^2V/s$ ,  $v_F = 10^8 m/s$ ,  $(\mu_+ + \mu_-)/2 = 0.5eV$ ,  $\mu_+ - \mu_- = 50meV$ , where  $\mu_{\pm}$  is the Fermi energy relative to the right/left-handed Weyl node, we get a large vortical current density of  $j = 100mA/mm^2$ . For  $q \sim 1/R$ , the above numbers result in the CVE (GVE) for  $\omega \ll 10^{11}$  Hz ( $\omega \gg 10^{11}$  Hz) Fig. 2(b) depicts a chiral Nernst effect, defined as

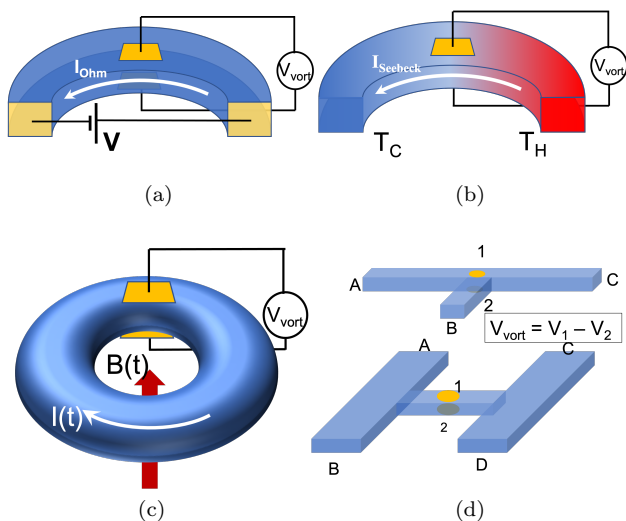


FIG. 2. Device geometries for utilizing the vortical effects. In (a), (b) and (c), respectively, a current is driven along a curved path by a voltage, a temperature gradient and a time-dependent magnetic field, which produces a vertical potential difference due to the vortical effects. In (d, top),  $V_{\text{vort}} \neq 0$  if a current is driven between  $AB$  or  $AC$  because it is forced to go around a corner, but  $V_{\text{vort}} = 0$  for a current between  $AC$ . (d, bottom) shows a more complex geometry with more terminals and corners that offers richer manipulation. Geometries in (d) can serve as building blocks for scalable circuits.

$\mathbf{j}(\mathbf{r}, t) \propto \nabla \times \nabla T(\mathbf{r})$ . Note,  $\nabla \times \nabla T$  is guaranteed to vanish only if  $T(\mathbf{r})$  is twice continuously differentiable on all space – a condition violated by the geometry of Fig. 2(b). Once again, we expect a large effect in WSMs owing to their large mobility. For  $\nabla T \sim 1\text{K}/\mu\text{m}$  and Seebeck coefficient  $S = 100\mu\text{V}/\text{K}$ , the resultant electric field is  $E = 0.1\text{V}/\text{m}$ , which leads to  $j = 100\text{mA}/\text{mm}^2$ . Fig. 2(d) shows examples of geometries that can form building blocks of larger circuits. Here, the vortical effects are invoked when the carriers have to turn a corner on their way from a source to a drain.

We thank the Department of Energy for funding this work via grant number DE-SC0022264. We are grateful to Shun-Chiao Chang, Zhao Huang, Daniel Bulmash, Karl Landsteiner and Liangzi Deng for insightful discussions.

[1] O. Vafek and A. Vishwanath, Annual Review of Condensed Matter Physics **5**, 83 (2014).  
 [2] A. A. Burkov, Annual Review of Condensed Matter Physics **9**, 359 (2018).  
 [3] A. A. Burkov, Nature Materials **15**, 1145 EP (2016).  
 [4] B. Yan and C. Felser, Annual Review of Condensed Matter Physics **8**, 337 (2017), arXiv:1611.04182.  
 [5] N. P. Armitage, E. J. Mele, and A. Vishwanath, Rev. Mod. Phys. **90**, 15001 (2018).

[6] S.-Q. Shen (2017).  
 [7] I. Belopolski, D. S. Sanchez, Y. Ishida, X. Pan, P. Yu, S.-Y. Xu, G. Chang, T.-R. Chang, H. Zheng, N. Alidoust, G. Bian, M. Neupane, S.-M. Huang, C.-C. Lee, Y. Song, H. Bu, G. Wang, S. Li, G. Eda, H.-T. Jeng, T. Kondo, H. Lin, Z. Liu, F. Song, S. Shin, and M. Z. Hasan, Nature Communications **7**, 13643 (2016).  
 [8] Z. P. Guo, P. C. Lu, T. Chen, J. F. Wu, J. Sun, and D. Y. Xing, Science China: Physics, Mechanics and Astronomy 10.1007/s11433-017-9126-6 (2018).  
 [9] G. Chang, S.-Y. Xu, H. Zheng, C.-C. Lee, S.-M. Huang, I. Belopolski, D. S. Sanchez, G. Bian, N. Alidoust, T.-R. Chang, C.-H. Hsu, H.-T. Jeng, A. Bansil, H. Lin, and M. Z. Hasan, Phys. Rev. Lett. **116**, 66601 (2016).  
 [10] A. Gyenis, H. Inoue, S. Jeon, B. B. Zhou, B. E. Feldman, Z. Wang, J. Li, S. Jiang, Q. D. Gibson, S. K. Kushwaha, J. W. Krizan, N. Ni, R. J. Cava, B. A. Bernevig, and A. Yazdani, New Journal of Physics **18**, 105003 (2016).  
 [11] S.-M. Huang, S.-Y. Xu, I. Belopolski, C.-C. Lee, G. Chang, B. Wang, N. Alidoust, G. Bian, M. Neupane, C. Zhang, S. Jia, A. Bansil, H. Lin, and M. Z. Hasan, Nature Communications **6**, 7373 (2015).  
 [12] H. Inoue, A. Gyenis, Z. Wang, J. Li, S. W. Oh, S. Jiang, N. Ni, B. A. Bernevig, and A. Yazdani, Science **351**, 1184 (2016).  
 [13] B. Q. Lv, N. Xu, H. M. Weng, J. Z. Ma, P. Richard, X. C. Huang, L. X. Zhao, G. F. Chen, C. E. Matt, F. Bisti, V. N. Strocov, J. Mesot, Z. Fang, X. Dai, T. Qian, M. Shi, and H. Ding, Nature Physics **11**, 724 EP (2015).  
 [14] Y. Sun, S. C. Wu, and B. Yan, Physical Review B - Condensed Matter and Materials Physics 10.1103/PhysRevB.92.115428 (2015).  
 [15] A. S.-y. Xu, I. Belopolski, N. Alidoust, M. Neupane, C. Zhang, R. Sankar, G. Chang, Z. Yuan, C.-c. Lee, S.-m. Huang, H. Zheng, J. Ma, D. S. Sanchez, B. Wang, F. Chou, P. P. Shibayev, H. Lin, S. Jia, and M. Zahid, Science (2015).  
 [16] S. Y. Xu, I. Belopolski, D. S. Sanchez, M. Neupane, G. Chang, K. Yaji, Z. Yuan, C. Zhang, K. Kuroda, G. Bian, C. Guo, H. Lu, T. R. Chang, N. Alidoust, H. Zheng, C. C. Lee, S. M. Huang, C. H. Hsu, H. T. Jeng, A. Bansil, T. Neupert, F. Komori, T. Kondo, S. Shin, H. Lin, S. Jia, and M. Z. Hasan, Physical Review Letters **116**, 096801 (2016), arXiv:1510.08430.  
 [17] S.-Y. Xu, I. Belopolski, N. Alidoust, M. Neupane, G. Bian, C. Zhang, R. Sankar, G. Chang, Z. Yuan, C.-C. Lee, S.-M. Huang, H. Zheng, J. Ma, D. S. Sanchez, B. Wang, A. Bansil, F. Chou, P. P. Shibayev, H. Lin, S. Jia, and M. Z. Hasan, Science **349**, 613 (2015).  
 [18] L. X. Yang, Z. K. Liu, Y. Sun, H. Peng, H. F. Yang, T. Zhang, B. Zhou, Y. Zhang, Y. F. Guo, M. Rahn, D. Prabhakaran, Z. Hussain, S. K. Mo, C. Felser, B. Yan, and Y. L. Chen, Nature Physics **11**, 728 EP (2015).  
 [19] H. Zheng, S. Y. Xu, G. Bian, C. Guo, G. Chang, D. S. Sanchez, I. Belopolski, C. C. Lee, S. M. Huang, X. Zhang, R. Sankar, N. Alidoust, T. R. Chang, F. Wu, T. Neupert, F. Chou, H. T. Jeng, N. Yao, A. Bansil, S. Jia, H. Lin, and M. Z. Hasan, ACS Nano **10**, 1378 (2016).  
 [20] H. B. Nielsen and M. Ninomiya, Physics Letters B **130**, 389 (1983).  
 [21] H. B. Nielsen and M. Ninomiya, Nuclear Physics B **185**, 20 (1981).  
 [22] H. B. Nielsen and M. Ninomiya, Nuclear Physics B **193**, 173 (1981).

- [23] P. Hosur and X. Qi, *Comptes Rendus Physique* **14**, 10.1016/j.crhy.2013.10.010 (2013).
- [24] H. Wang and J. Wang, *Chinese Physics B* **27**, 107402 (2018).
- [25] J. Hu, S.-Y. Xu, N. Ni, and Z. Mao, *Annual Review of Materials Research* **49**, 207 (2019).
- [26] A. A. Zyuzin and A. A. Burkov, *Phys. Rev. B* **86**, 115133 (2012).
- [27] Y. Chen, S. Wu, and A. A. Burkov, *Phys. Rev. B* **88**, 125105 (2013).
- [28] M. M. Vazifeh and M. Franz, *Phys. Rev. Lett.* **111**, 27201 (2013).
- [29] A. A. Burkov, *Journal of Physics: Condensed Matter* **27**, 113201 (2015).
- [30] P. Hosur, S. Parameswaran, and A. Vishwanath, *Physical Review Letters* **108**, 10.1103/PhysRevLett.108.046602 (2012).
- [31] F. de Juan, A. G. Grushin, T. Morimoto, and J. E. Moore, *Nature Communications* **8**, 15995 (2017).
- [32] S. Wang, B. C. Lin, A. Q. Wang, D. P. Yu, and Z. M. Liao, *Advances in Physics: X* **2**, 518 (2017).
- [33] N. Nagaosa, T. Morimoto, and Y. Tokura, *Nature Reviews Materials* **5**, 621 (2020).
- [34] M. V. Isachenkov and A. V. Sadofyev, *Physics Letters B* **697**, 404 (2011).
- [35] A. V. Sadofyev, V. I. Shevchenko, and V. I. Zakharov, *Phys. Rev. D* **83**, 105025 (2011).
- [36] P. Goswami and S. Tewari, *Phys. Rev. B* **88**, 245107 (2013).
- [37] Z. Wang and S.-C. Zhang, *Phys. Rev. B* **87**, 161107 (2013).
- [38] G. Basar, D. E. Kharzeev, and H.-U. Yee, *Phys. Rev. B* **89**, 35142 (2014).
- [39] K. Landsteiner, *Phys. Rev. B* **89**, 75124 (2014).
- [40] R. Loganayagam and P. Surówka, *Journal of High Energy Physics* **2012**, 97 (2012).
- [41] A. Vilenkin, *Phys. Rev. D* **21**, 2260 (1980).
- [42] D. E. Kharzeev, *Progress in Particle and Nuclear Physics* **75**, 133 (2014).
- [43] A. A. Zyuzin, S. Wu, and A. A. Burkov, *Phys. Rev. B* **85**, 165110 (2012).
- [44] P. Goswami and S. Tewari, Chiral magnetic effect of weyl fermions and its applications to cubic noncentrosymmetric metals (2013), arXiv:1311.1506 [cond-mat.mes-hall].
- [45] M.-C. Chang and M.-F. Yang, *Phys. Rev. B* **91**, 115203 (2015).
- [46] M.-C. Chang and M.-F. Yang, *Phys. Rev. B* **92**, 205201 (2015).
- [47] P. Goswami and A. H. Nevidomskyy, *Phys. Rev. B* **92**, 214504 (2015).
- [48] S. Zhong, J. E. Moore, and I. Souza, *Phys. Rev. Lett.* **116**, 077201 (2016).
- [49] D. T. Son and N. Yamamoto, *Phys. Rev. Lett.* **109**, 181602 (2012).
- [50] A. Vilenkin, *Phys. Rev. Lett.* **41**, 1575 (1978).
- [51] A. Vilenkin, *Physics Letters B* **80**, 150 (1978).
- [52] A. Vilenkin, *Phys. Rev. D* **20**, 1807 (1979).
- [53] A. Vilenkin, *Phys. Rev. D* **22**, 3067 (1980).
- [54] O. V. Rogachevsky, A. S. Sorin, and O. V. Teryaev, *Phys. Rev. C* **82**, 054910 (2010).
- [55] M. A. Stephanov and Y. Yin, *Phys. Rev. Lett.* **109**, 162001 (2012).
- [56] J.-Y. Chen, D. T. Son, M. A. Stephanov, H.-U. Yee, and Y. Yin, *Phys. Rev. Lett.* **113**, 182302 (2014).
- [57] G. Y. Prokhorov, O. V. Teryaev, and V. I. Zakharov, *Phys. Rev. D* **98**, 071901 (2018).
- [58] G. Prokhorov and O. Teryaev, *Phys. Rev. D* **97**, 076013 (2018).
- [59] G. Y. Prokhorov, O. V. Teryaev, and V. I. Zakharov, *Journal of High Energy Physics* **2019**, 146 (2019).
- [60] V. I. Zakharov and O. V. Teryaev, Quark-hadron duality in hydrodynamics: an example (2018), arXiv:1801.08183 [hep-th].
- [61] M. Stone and J. Kim, *Phys. Rev. D* **98**, 025012 (2018).
- [62] D. E. Kharzeev, J. Liao, S. A. Voloshin, and G. Wang, *Progress in Particle and Nuclear Physics* **88**, 1 (2016).
- [63] A. Shitade, K. Mameda, and T. Hayata, *Phys. Rev. B* **102**, 205201 (2020).
- [64] R. Toshio, K. Takasan, and N. Kawakami, *Phys. Rev. Research* **2**, 032021 (2020).
- [65] Z. V. Khaidukov, V. P. Kirilin, and A. V. Sadofyev, *Physics Letters B* **717**, 447 (2012).
- [66] V. P. Kirilin, A. V. Sadofyev, and V. I. Zakharov, *Phys. Rev. D* **86**, 25021 (2012).
- [67] D. Bohm, *Phys. Rev.* **75**, 502 (1949).
- [68] Y. Ohashi and T. Momoi, *Journal of the Physical Society of Japan* **65**, 3254 (1996), <https://doi.org/10.1143/JPSJ.65.3254>.
- [69] N. Yamamoto, *Phys. Rev. D* **92**, 085011 (2015).
- [70] H. Watanabe, *Journal of Statistical Physics* **177**, 717 (2019).